REPORT DOCUMENTATION PAGE		Form Approved OMB No. 0704-0188

Public reporting burden for this collection of information is estimated to average 1 hour per response, including the time for reviewing instructions, searching existing data sources, gathering and maintaining the data needed, and completing and reviewing the collection of information. Send comments regarding this burden estimate or any other aspect of this collection of information, including suggestions for reducing this burden, to Washington Headquarters Services, Directorate for Information Operations and Reports, 1215 Jefferson Davis Highway, Suite 1204, Arlington, VA 22202-4302, and to the Office of Management and Budget, Paperwork Reduction Project (0704-0188), Washington, DC 20503.

1. AGENCY USE ONLY *(Leave blank)*	2. REPORT DATE 30-Sep 97	3. REPORT TYPE AND DATES COVERED

4. TITLE AND SUBTITLE
INVESTIGATING THE EFFECTS OF CORROSION ON THE FATIGUE LIFE OF STEEL

5. FUNDING NUMBERS

6. AUTHOR(S)
Todd S. Waldvogel

7. PERFORMING ORGANIZATION NAME(S) AND ADDRESS(ES)
UNITED STATES AIR FORCE ACADEMY

8. PERFORMING ORGANIZATION REPORT NUMBER
97-032

9. SPONSORING/MONITORING AGENCY NAME(S) AND ADDRESS(ES)
THE DEPARTMENT OF THE AIR FORCE
AFIT/CIA
2950 P STREET
WPAFB OH 45433

10. SPONSORING/MONITORING AGENCY REPORT NUMBER

11. SUPPLEMENTARY NOTES

12a. DISTRIBUTION AVAILABILITY STATEMENT

DISTRIBUTION STATEMENT A
Approved for public release
Distribution Unlimited

12b. DISTRIBUTION CODE

13. ABSTRACT *(Maximum 200 words)*

DTIC QUALITY INSPECTED 4

14. SUBJECT TERMS

15. NUMBER OF PAGES
55

16. PRICE CODE

17. SECURITY CLASSIFICATION OF REPORT	18. SECURITY CLASSIFICATION OF THIS PAGE	19. SECURITY CLASSIFICATION OF ABSTRACT	20. LIMITATION OF ABSTRACT

ABSTRACT

Investigating the Effects of Corrosion on the Fatigue Life of Steel. (August 1997)
Todd S. Waldvogel, B.S., United States Air Force Academy
Chair of Advisory Committee: Dr. Peter B. Keating

Given the vast size of this country's vast infrastructure and the increasingly competitive environment for fiscal support, it is important that maintenance funds be appropriately allocated. Many structural components of our infrastructure are affected by the corrosion process. By most accounts, corrosion is typically considered to provide only negative effects on structural systems. Argument can be made, however, that corrosion may in fact deter fatigue crack initiation in low stress cyclic loading.

A testing procedure to investigate the effects of corrosion on the fatigue life of steel is established, completed, and evaluated. Twenty-four steel specimens are immersed in saltwater solution and removed on intervals for repetitive loading. Once tested, the surviving specimens are returned to the saline solution. This process is continued until each specimen fails. The results show that 22 of 24 corroded specimens had higher mean fatigue lives than the mean non-corroded fatigue life when subjected to this intermediate corrosion and low stress range cyclic tension loading.

REFERENCES

Albrecht, Pedro, "Fatigue Design Stresses for Weathering Steel Structures," *Corrosion Fatigue: Mechanics, Metallurgy, Electrochemistry, and Engineering, ASTM STP 801*, pp. 445-471, 1983.

Barsom, John M. & Stanley T. Rolfe, Fracture and Fatigue Control in Structures, 2nd ed., 1987.

Boresi, Arthur P., Richard J. Schmidt & Omar M. Sidebottom, Advanced Mechanics of Materials, 5th ed., 1993.

Fisher, J., "Fatigue Resistance of Weathering Steel Components", Forum on Weathering Steel for Highway Structures: Summary Report, June 1989.

Harrison, J.D, "An analysis of data on non-propagating fatigue cracks on a fracture mechanics basis," *Metal Construction and British Welding Journal*, March, 1970.

Mattsson, Einar, Basic Corrosion Technology for Scientists and Engineers, 1989.

Ohta, Akihiko, Takeshi Kono, & Satoshi Nishijima, "Near-threshold Fatigue Crack Propagation of Welded Joint Under Varying Loading," *Engineering Fracture Mechanics* Vol. 21, No3, pp. 521-528, 1985.

Wright, William J., & Pedro Albrecht, "Fatigue Crack Growth Rates in Bridge Steels," *Transportation Research Record 1290*.

INVESTIGATING THE EFFECTS OF CORROSION ON THE FATIGUE LIFE

OF STEEL

A Major Report

by

TODD S. WALDVOGEL

in partial fulfillment of the requirements for the degree of

MASTER OF ENGINEERING

August 1997

Major Subject: Civil Engineering

ABSTRACT

Investigating the Effects of Corrosion on the Fatigue Life of Steel. (August 1997)

Todd S. Waldvogel, B.S., United States Air Force Academy

Chair of Advisory Committee: Dr. Peter B. Keating

Given the size of this country's vast infrastructure and the increasingly competitive environment for fiscal support, it is important that maintenance funds be appropriately allocated. Many structural components of our infrastructure are affected by the corrosion process. By most accounts, corrosion is typically considered to provide only negative effects on structural systems. Argument can be made, however, that corrosion may in fact deter fatigue crack initiation in low stress cyclic loading.

A testing procedure to investigate the effects of corrosion on the fatigue life of steel is established, completed, and evaluated. Twenty-four steel specimens are immersed in a saltwater solution and removed on intervals for repetitive loading. Once tested, the surviving specimens are returned to the saline solution. This process is continued until each specimen fails. The results show that 22 of 24 corroded specimens had higher mean fatigue lives than the mean non-corroded fatigue life when subjected to this intermediate corrosion and low stress range cyclic tension loading.

ACKNOWLEDGEMENTS

TABLE OF CONTENTS

LIST OF FIGURES

LIST OF TABLES

CHAPTER I

Introduction

1.1 Background

Concerns with the safety of the country's infrastructure continue to grow. Corrosion affects many components of the infrastructure, such as steel highway bridges. Past research has shown that a corroded bridge member that has previously been in service for years will quickly develop fatigue cracks when removed from service and subject to laboratory repetitive loading. However, the laboratory setting may result in an unrealistic fatigue damage accumulation due to the absence of the continued on-going corrosion process. From these test results, it has been suggested that the fatigue strength of corroded in-service steel bridge members be reduced when assessing the members' remaining service life. This conclusion, if implemented, would have a serious impact on the allocation of limited funds for infrastructure rehabilitation.

Examining the performance of existing in-service and weathering bridges, however, shows that fatigue cracks do not develop from corrosion unless the corrosion is so severe that the member's cross section has been reduced by 50 percent or more. It is theorized that the corrosion process consumes the developing crack and, hence, the crack is never able to establish itself unless the localized stress range is significantly increased due to the reduction in cross sectional area.

1.2 Research Objectives

The objective of this study is to validate a fatigue testing methodology that more closely simulates the coupling of the corrosion process with fatigue crack growth. Small-scale steel specimens were alternately (and separately) cycle fatigue loaded and corroded. By changing both the number of applied load cycles in the interval and the length of time the specimen is immersed in a sodium chloride bath between load cycling, a more realistic fatigue damage accumulation process will result. As a consequence, the tests results should be more consistent with observed field behavior, allowing for a better prediction of fatigue lives of bridge components.

CHAPTER II

Fatigue & Corrosion

2.1 Overview

In determining the remaining service life for constructed steel structures, two important issues of concern are fatigue and corrosion. In today's industry, there is some disagreement as to the relationship of these two deterioration processes. To investigate this issue, one must first understand the mechanics behind fatigue cracking and the factors (corrosion in particular) which effect service life. Once a correlation between corrosion and fatigue crack initiation is established, consideration must be given to what, if any, actions must be taken in evaluation of existing structures as well as in the design of new structures.

2.2 Fatigue

Fatigue is defined as a process of cumulative damage caused by repeated fluctuating loads (Barsom 1987). Barsom (1987) points out that damage from fatigue only occurs in regions that plastically deform under an applied fluctuating load. Such plastic deformations are possible even under elastic stress fluctuations in the presence of stress (or strain) raisers. Stress (strain) raisers are geometric configurations or imperfections which locally concentrate stress (strain) and accelerate it to a higher level than the applied elastic load. Fluctuation of local stress (strain) is the primary factor which affects the fatigue behavior of steel. The increased stress (strain) loads/fluctuations

at these locations provide the plastic environment necessary for the initiation of fatigue damage—cracks—after a certain number of load fluctuations.

The detrimental effect of cyclic loading on steel is the initiation and propagation of fatigue cracks. The transformation from initiation to propagation can be very difficult to identify. Once initiated, propagation of fatigue cracks beyond critical dimensions induce brittle fracture of the structure or specimen. Brittle fracture may occur at levels of stress below typical yielding conditions. This mechanism of failure is not desirable as the slow failure associated with large plastic deformations and yielding rate, which provides "running time," will not be present. Once a fatigue crack is observed, it is important to assess the rate of growth of the crack and to predict the estimated life of the member so as to administer appropriate maintenance efforts.

2.3 Mechanics of Fatigue Crack Initiation

Crack initiation identifies the point at which a fatigue crack begins to develop. Once initiated, the crack may propagate with continued cyclic loading. A material's resistance to fatigue crack propagation can be represented by the relationship of the crack propagation rate, da/dN, and the stress intensity factor range ΔK (Ohta 1985). If this rate is plotted as a function of the stress intensity factor, ΔK in a log/log format, a graph similar to Figure 1 (Wright) can be constructed.
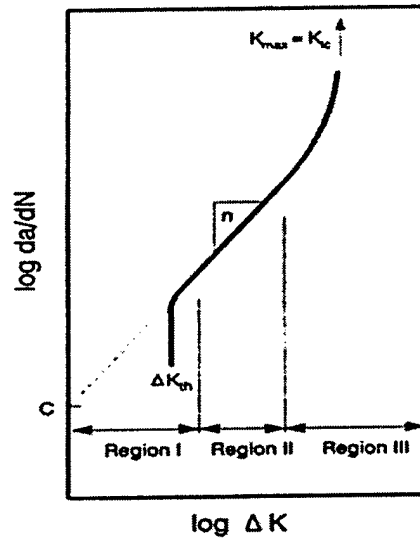
Figure 1. Fatigue crack growth vs. stress intensity factor range

This plot, which is independent of material strengths, reveals three distinct regions of

different relationships. At lower values of crack propagation rate, there exists a threshold

level, ΔK_{th}, below which the fatigue crack does not propagate. This behavior is

represented as Region I. Beyond this threshold, crack propagation occurs at different

rates. Within Region II the plot reveals a linear correlation between ΔK and da/dN. This

demonstrates the Paris power law where the fatigue crack propagation behavior can be

represented as:

$$\frac{da}{dN} = A(\Delta K)^m$$

where A and m are constants. Region III realizes an asymptotic increase of da/dN as

K_{max} approaches the fracture toughness, K_{Ic}.

For the purpose of this report, the emphasis shall be placed upon the relationships

near the threshold for crack propagation, ΔK_{th}. Some systems in real-world structural

applications, such as highway bridges, are repeatedly exposed to small stress ranges.

This low stress range corresponds with the low ΔK of Region I. For this reason, fatigue

crack initiation and sub-threshold propagation warrant investigation. For steel, this

threshold is estimated as:

$$\Delta K = 6.4(1 - 0.85R)$$

where the stress ratio, R, represents the ratio of the minimum stress to the maximum

stress (Barsom 1987).

2.4 Corrosion

Corrosion is typically defined as "the chemical or electrochemical reaction

between a material, usually a metal, and its environment that produces a deterioration of

the material and its properties" (ASM Metals Handbook, 1987). The corrosion of a metal

in an aqueous environment occurs when two or more electrochemical reactions take place

on the surface of the metal. As a result of this process, elements of the metal change from

a metallic to a simpler nonmetallic corrosion product. The degradation of iron (the

primary element of steel) into rust is a familiar example of this process.

The corrosion of metal requires simultaneous oxidation and reduction reactions.

In general, this process can be summarized by the following generic reaction:

$$M + O \rightarrow M^{n+} + R$$
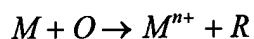
This demonstrates the dissolution of the metal ($M \rightarrow M^{n+}$) driven by the cathodic

reaction ($O \rightarrow R$), "where M is a metal, O is oxygen or another an oxidizing reagent, $n+$

is the multiple of the charge, and R is the reduced species or reduction" (ASM Metals

Handbook, 1987). These two reactions take place on two distinct sites on the same

surface as shown in Figure 2 (ASM Metals Handbook, 1987).
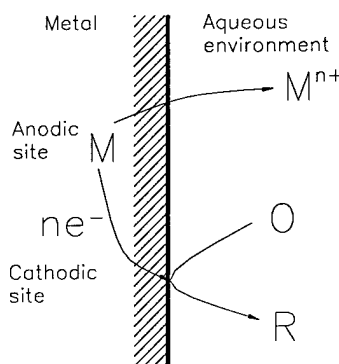
Figure 2. Schematic of corrosion process

It the case of steel, the electrochemical reactions destroy exposed outer layers of

steel. This destruction reduces the gross area of steel sections producing a negative affect

from nearly all elastic design approaches. These design procedures force failure as a

function of yield so as to promote significant plastic deformation upon failure to provide

ample visual warning of collapse, "running time." Accordingly, there is no wonder why

the term "corrosion" conjures a negative connotation.

Crevice corrosion will be a specific process expected in a specimen with a

notched area. This type of corrosion can exist when the area of a small surface notch

differs in environmental conditions. The geometry of a notch shields the immediate area

from circulating fluid and allows for the stagnation of the immediate notch environment.

Under such stationary conditions, the pH can decrease and the concentration of chloride

can increase both resulting in higher corrosivity inside of the notch than outside. Anodic

attack of the metal usually occurs near the mouth of the crevice, while cathodic reduction

of the oxygen from the surroundings takes place on the metal surface outside as depicted

in the following reactions and Figure 3 (Mattsson 1989):

Anode reaction: $Me \rightarrow Me^{n+} + ne^-$

Cathode reaction: $\frac{1}{2}O_2 + H_2O + 2e^- \rightarrow 2OH^-$
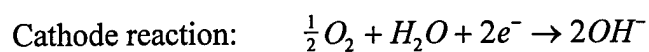
The phenomenon of crevice corrosion helps explain the greater corrosion losses at the

notch than at the specimen surface.
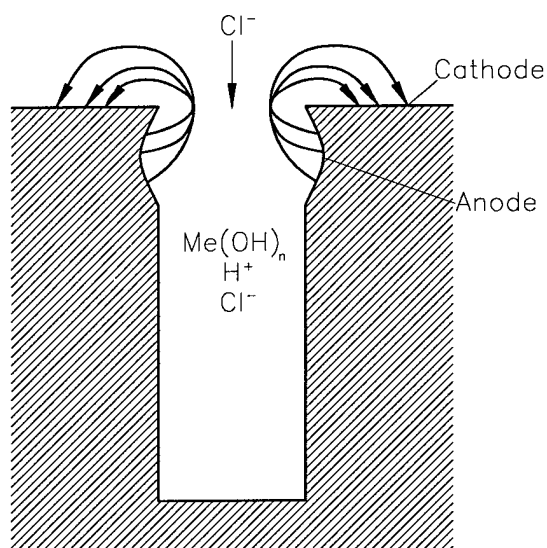
Figure 3. Crevice corrosion

2.5 Correlation of Corrosion and Fatigue Crack Initiation

How does corrosion affect initiation and propagation of fatigue cracks? Experts

in the field cannot even agree to disagree. There are two strikingly opposite opinions,

each based upon testing and field experience.

2.5.1 "Corrosion reduces fatigue life..."

One school of thought believes "weathering consumes the crack initiation life"

(Albrecht 1983). Basically the argument is that the introduction of surface defects

through corrosive pitting initiates a crack and that from this point forward, crack

propagation is of concern. The initiation of the crack is a function of the corrosion as

well as of the loading condition, hence cracks may initiate without any occurrence of

fluctuating stress. "Unpainted weathering steel structures exposed to atmospheric

environments lose initiation life due to rust pitting and propagation life due to corrosion

fatigue" (Albrecht 1983). Referring to surface irregularities caused by corrosion pitting,

Barsom (1987) states, "The fatigue-crack-initiation life of a notched specimen can be

reduced significantly by surface irregularities in the vicinity of the notch tip" (1987).

Such beliefs cause apprehension when considering the large number of

constructed steel facilities in service across the United States and throughout the world.

"Corrosion fatigue damage occurs more rapidly than would be expected from the

individual effects or from the algebraic sum of the individual effects of fatigue, corrosion,

or stress-corrosion cracking" (Barsom 1987). So why then is it that with this large

number of steel structures exposed to weathering that more failures attributed to fatigue

cracking and brittle failure have not occurred? Is it possible that this school of thought is

incorrect? Such consideration certainly seems plausible—or at least that it is not entirely correct.

2.5.2 "Corrosion increases fatigue life..."

The second school of thought decidedly disagrees with the opinion of Albrecht. In fact, some experts are even willing to say that corrosion of steel may improve the resistance to crack initiation of steel *subjected to low-stress fluctuating loads*. A study performed by Bucci and Donald in 1972 demonstrated such a phenomenon (Barsom 1987). According to Bucci and Donald, submergence of a steel specimen in "salt water appears to produce an inhibitive effect of fatigue cracking at the very low ΔK_{th} levels" (Barsom 1987). In another instance provided by Barsom (1987), "the value of the ΔK_{th} in the A514 steels tested at 12 cpm in 3 percent sodium chloride solution was twice as large as the value of 5.5 ksi in$^{1/2}$ (6.0 MN/m$^{3/2}$) for room temperature air." In yet a third instance, Kentro Yamada of Nagoya provided an oral report on weathered steel stiffener and attachment specimens at the International Association for Bridge and Structural Engineering (IABSE) Colloquium on Fatigue of Steel and Concrete Structures held in Lausanne in March 1982, stating that five-year weather specimens provided equal or greater fatigue resistance than the original nonweathered control specimens (Fisher 1989). This fatigue resistance can only be attributed to reduced rates of crack initiation and propagation.

2.5.3 Theoretical evaluation

A mathematical investigation of the equation for ΔK supports the second school of thought. Barsom (1987) shows that a generic equation for the range of the stress intensity factor is represented by:

$$\Delta K = \Delta\sigma\sqrt{a\pi} \times f(g)$$

where $f(g)$ encompasses the appropriate specimen and crack geometry. For any given situation, a load condition will be predicted and $f(g)$ will depend on the geometry. With this in mind, the only remaining factor is the depth of the initiating crack itself. The only way to affect ΔK in a given geometry with a given stress range is to manipulate the depth of the crack, a. Corrosion may just be capable of providing this manipulation.

Through corrosion, the outermost layer of steel is deteriorated. What if the layer of steel that contained a crack attempting to initiate was destroyed? Continuing with this line of thought, what if the member were to continue corroding at a rate greater than that of crack initiation? The scale at issue is so small compared to specimen geometry than it will be said $f(g)$ does not change. Certainly the net area of the specimen is reduced, and this should trigger some concern. But if the crack can be "removed" then the specimen is returned to a condition where it will fail by yielding rather than brittle fracture.

2.6 Design Implications

The design implications of fatigue-corrosion interaction depend on which theory is considered "correct." "The life of the component can be prolonged by extending the crack-initiation life and the subcritical-crack-propogation life. Consequently, crack initiation, subcritical crack propagation, and fracture characteristics of structural materials are primary considerations in the formulation of fracture-control guidelines for structures" (Barsom 1987). Barsom goes on to say "...discontinuities in large complex structures may...initiate under cyclic loads...The designer must properly proportion the structure to prevent failure by either tensile overload or comprehensive instability and by unstable crack growth by brittle fracture" (1987).

One engineer may argue that the fatigue resistance of weathering steel should be reduced. Albrecht (1983) proposes fatigue life reductions. He says that a crack will propagate, thereby inferring brittle fracture and he recommends examining "the safety margin against fatigue of highway bridges designed to current AASHTO specifications in terms of the lower allowable stress ranges proposed herein" (Albrecht 1983). Albrecht (1983) is not alone in his conclusion: the British rules for the design of fixed offshore structures reduce the fatigue limit to allow for seawater corrosion. However, some regard this reduction as an unnecessary, inefficient precaution, which can be supported by the previously presented results. Cracks can exist without propagating under fatigue loading (Harrison 1970). And in actual structures, Fisher (1989) noted that cracks are seldom observed at the corrosion notched specimen until a section loss of greater than 50 percent occurs. Fisher (1989) attributes this to the fact that corrosion rates exceed the rates of

fatigue damage and that any damage due to cyclic loading appears to be removed by the ongoing corrosion process. Fisher and Yamada each tested corroded steel connections, independently, and realized results consistently demonstrating higher fatigue resistance than dictated by current AASHTO codes.

CHAPTER III

Experimental Testing

3.1 Experimental Research

In order to investigate the correlation between corrosion and fatigue crack initiation, notched steel tension specimens were subjected to alternating periods of accelerated corrosion and low stress range repetitive loading. Evaluation of the resulting fatigue failure will help provide insight into the effects of corrosion upon fatigue crack initiation in steel.

3.2 Experimental set-up

3.2.1 Specimen properties

Steel tension specimens, fabricated from ASTM A36 3/16" X 2" bar stock, were used. The geometry of all specimens tested were identical to that presented in Figure 4. The notch in the center of the specimen was used to induce a stress concentration with a reproducible fatigue strength. This notch was machined to a depth of $1/32^{nd}$ of an inch with a groove angle of 40 degrees. The area around the notch was sandblasted to remove the mill scale and isolate the corrosion process to a confined area.

8.0"

2.0"   4.0"   2.0"

2.0"

1.0"

2.0"

0.5" rad.
(Typ.)

Machined notch
(near side only)

Region to be cleaned
and free of mill-scale
(near side only)

Notes:
   All material 3/16" ASTM A36 bar
stock.
   Milled edges to be ground smooth.
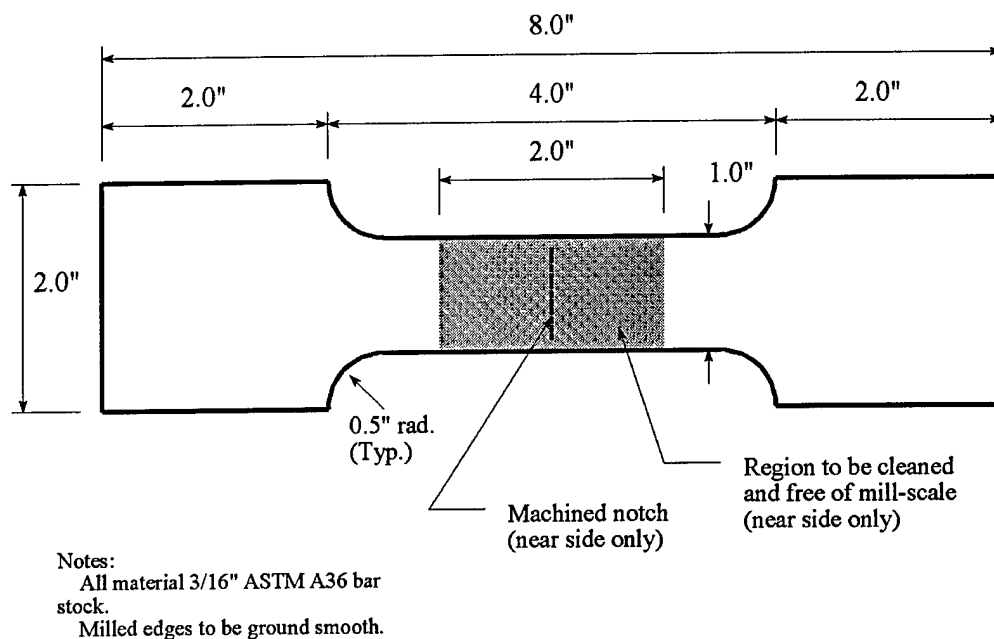
Figure 4. Specimen geometry

3.2.2 Control specimens (Strength and fatigue life)

Three specimens, one from each 20 foot length of bar stock, were tested in tension

(see Figure 5) to determine the yield and ultimate strengths of the steel. The plotted

stress-strain results of these tests are presented as Figure 6.   As indicated by the stress-

strain plots in Figure 6, specimens B & C showed similar stress-strain behavior. It was

assumed that similar stress-strain behavior is indicative of similar chemical

characteristics. The bar stock for these two specimens were used to fabricate all of the

corrosion specimens used in the test program. The specimens exhibited yield strengths of

approximately 60 ksi, much higher yield than their 36ksi designation, and an ultimate

strength of over 80 ksi.

Figure 5. Specimen in tension

Figure 6. Yield test results

approximately 60 ksi, much higher yield than their 36ksi designation, and an ultimate

strength of over 80 ksi.

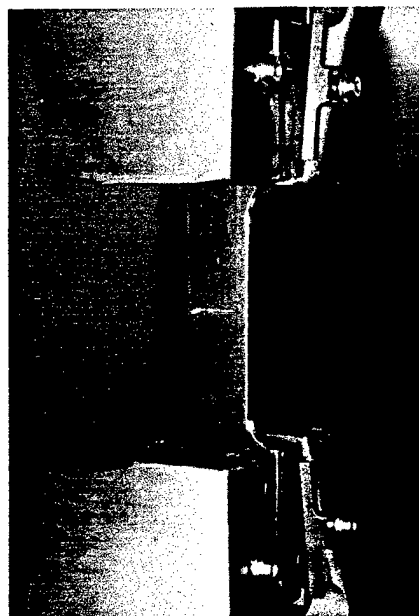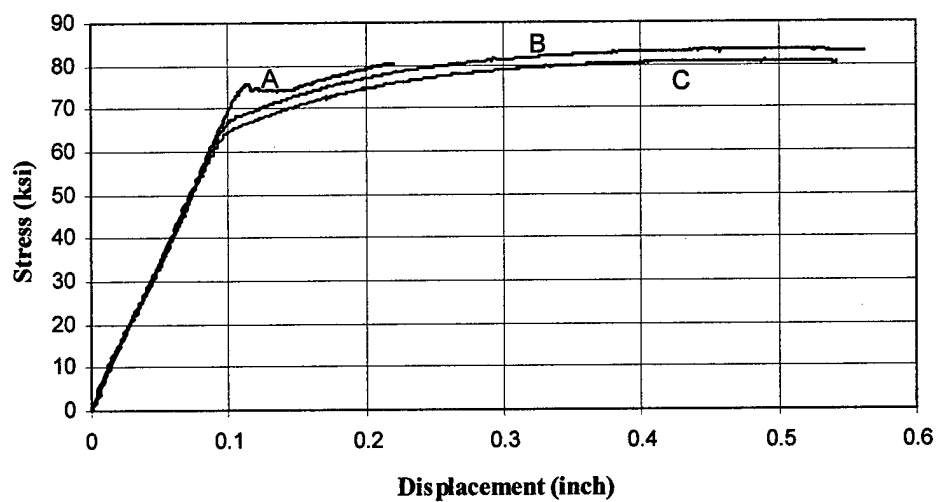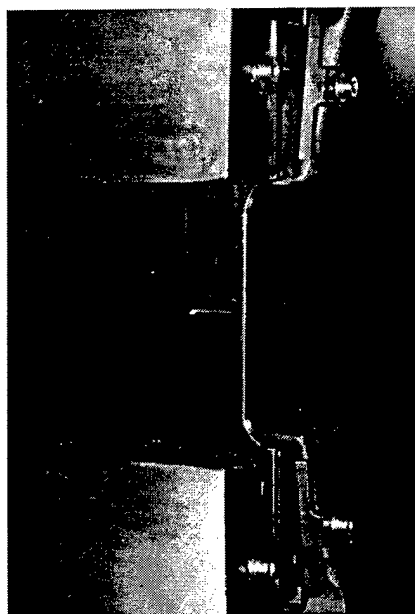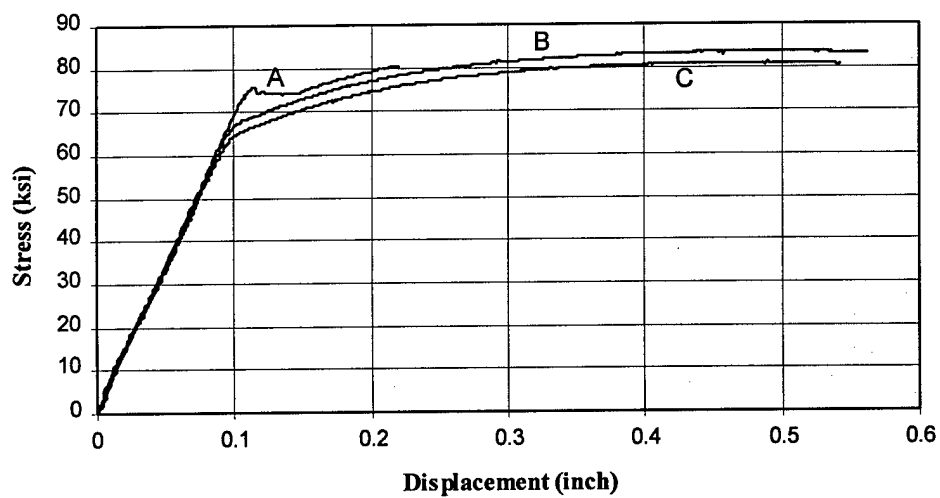**Figure 5. Specimen in tension**

Figure 6. Yield test results

Baseline testing was performed to establish the mean fatigue life of the specimens when subjected to repetitive loading in the absence of a corrosive environment. To maintain consistent loading conditions, a cyclic tension load was applied to induce a nominal stress range of 35 ksi and a minimum stress level of 10 ksi (and thereby a maximum of 45ksi) at a loading rate of 20 Hz. This range provides, according to the relationship provided earlier, provides a ΔK_{th} value of 5.19 ksi$\sqrt{in}$

This tension-tension load cycle was utilized to minimize the effects of crack closure. Grossly simplified, if the specimen were to go into compression, any developing crack would close and the compression would not propagate the crack. (In reality, the compression cycle would have effects on the crack, but not as significant as those of the tension cycle.) Under alternating conditions of compression and tension, only the range in the tension cycle would be used to calculate ΔK. Therefore, by utilizing only a cyclic tension load, the stress range is maximized and an upper bound of crack growth is provided by this experiment. Additionally, if corrosion debris were to become present within a crack, the crack would not be able to close completely in the compressive cycle. Such an occurrence could increase the compressive range and decrease the tension range in an unpredictable manner.

This cyclic loading was accomplished until failure of the notched specimens by fatigue crack propagation and ductile fracture. The results of this fatigue life control testing are shown in Table 1. As indicated by the cycles to failure in Table 1, the fatigue lives of three of the specimens were in close agreement. The mean fatigue life was taken as the average of specimens 1, 3, and 4. Specimen 2 was excluded because it was so

much greater than the close grouping of the other three. This may be accounted for by a slight camber that could have decreased the stresses at the notch tip. Excluding specimen 2, the fatigue life averaged 41,000 cycles. For the purpose of future comparison, the average fatigue life was also calculated including the failure of specimen 2. Including specimen 2 would increase the average fatigue life to 47,150 cycles.

Control Specimen	Cycle count
1	40,960
2	66,427
3	39,576
4	41,642

Table 1. Control fatigue lives

3.2.3 Test Environments

Twenty-four specimens comprised the test groups. These specimens were subjected to accelerated corrosion in a salt water bath. For each of two specimen groups, two gallons of distilled water were converted to a 3.5% salt solution by weight through the addition of 0.58 pounds of sodium chloride (NaCl), an environment similar to clean seawater (Mattsson 1989). This solution was thoroughly mixed and continually aerated and agitated with the assistance of a small aquarium air pump. The diagram in Figure 7 and the photograph in Figure 8 illustrate the set-up of the corrosive environment.

Figure 7. Set-up of corrosive environment

Figure 8. View of experimental set-up

Two similar environments were created to facilitated two major test groups based upon submersion time. The first group remained in the solution in one week intervals (160 hours), while the second group remained in solution for one half week intervals (72 hours). For the sake of easy referral, these groups shall be referred to as groups 1 and 2 of the *exposure index*, respectively.

Within each of the two *exposure* groups were twelve specimens. This group of twelve specimens is further divided into four sub-group sets based upon loading conditions. Set 1 was subjected to 50% (20,500 cycles) of the projected fatigue life; set
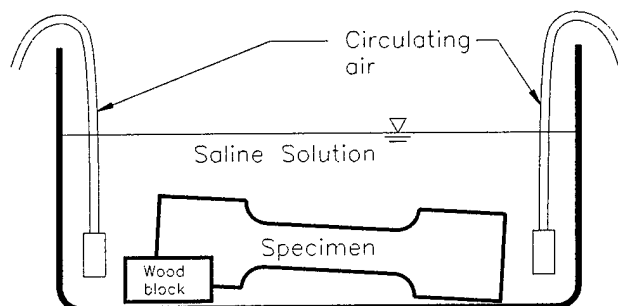
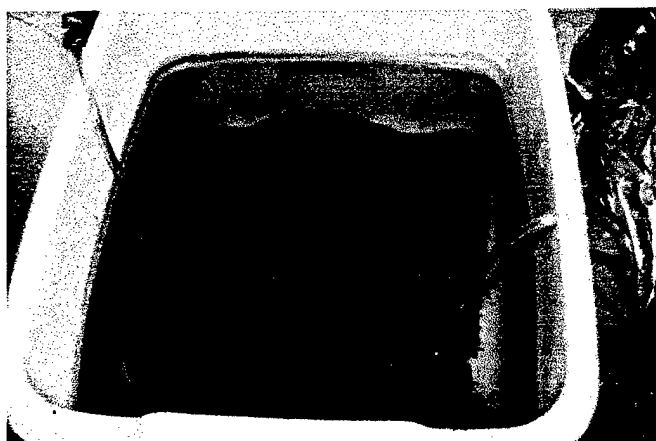**Figure 7. Set-up of corrosive environment**
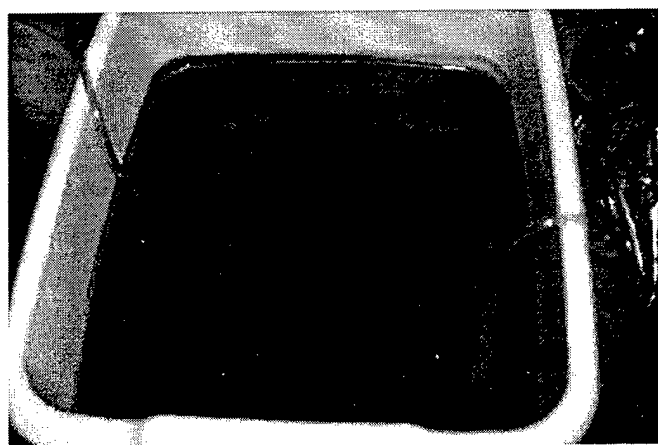
Figure 8. View of experimental set-up

Two similar environments were created to facilitated two major test groups based upon submersion time. The first group remained in the solution in one week intervals (160 hours), while the second group remained in solution for one half week intervals (72 hours). For the sake of easy referral, these groups shall be referred to as groups 1 and 2 of the *exposure index*, respectively.

Within each of the two *exposure* groups were twelve specimens. This group of twelve specimens is further divided into four sub-group sets based upon loading conditions. Set 1 was subjected to 50% (20,500 cycles) of the projected fatigue life; set
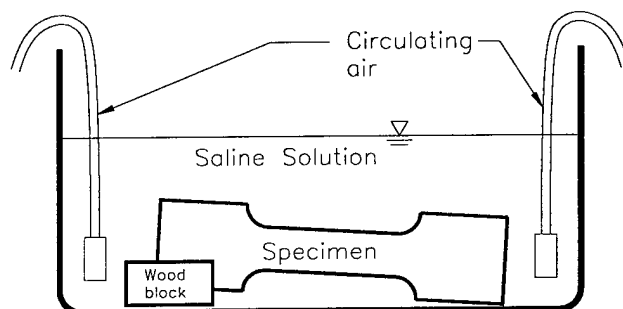
2 was subjected to 25% (12,250 cycles), set 3 to 12.5% (6,125 cycles) and set 4 to 6.25% (2,560 cycles). For easy referral, these sets shall be referenced as the *load indices* 1, 2, 3, and 4.

Specimen Identification	$\%(N_f)_{mean}$	$N_{interval}$
1-1-n	50%	20,500
1-2-n	25%	10,250
1-3-n	12.5%	5,130
1-4-n	6.25%	2,560

Table 2. Specimen identification, Exposure Index 1

Specimen Identification	$\%(N_f)_{mean}$	$N_{interval}$
2-1-n	50%	20,500
2-2-n	25%	10,250
2-3-n	12.5%	5,130
2-4-n	6.25%	2,560

Table 3. Specimen identification, Exposure Index 2

Within each of these load sets there were three specimens. As a result, the specimens shall be referred to by the exposure index, the load index, and the specimen number (1, 2, or 3): *exposure index-load index-specimen number*. For example, the notation *1-3-2* indicates that the specimen is the second of three subjected to week-long exposure and 12.5% loading. This identification process is presented in tabular formats in Tables 2 & 3.

3.2.4 Control specimens (Corrosion rate)

In addition to the 24 fatigue specimens, four specimens were corroded simultaneously with the group of *exposure index 1* specimens. The first of the four specimens was not returned to the solution after the first corrosion interval. The second underwent two 160 hour corrosion intervals, the third four, and the fourth eight. They did not undergo any loading between exposure intervals and served only to document corrosion rates and the degree of pitting within the notch.

3.3 Testing Procedure

The testing proceeded as follows. At each scheduled interval (160 hours or 72 hours) the twelve specimens were removed from solution, cleaned, and dried with compressed air prior to load application. Each specimen was then subjected to the appropriate percentage of tension load cycles based on its load index. This repetitive testing proceeded until each of the specimens had failed and provided a fatigue life to be compared with the average 41,000 cycle life. Upon completion of tensile loading, any surviving specimens were returned to a freshly prepared saltwater solution for another exposure cycle.

Each of the two exposure groups began with one week of corrosion prior to any load application. This exposure does not affect the outcomes based upon different exposure times because the specimens had not been subjected to any cyclic loading that would initiate fatigue cracking.

3.4 Corrosion loss measurements

Corrosion rates were calculated using initial and final thicknesses of the test specimens. Once the specimen had failed, the mill scale was sandblasted off of the back side behind the previously blasted area where corrosion occurred. This allowed for a true loss without consideration of the mill scale. To establish the initial thickness, two areas protected by the mill scale from corrosion were sandblasted. A thickness measurement taken here represents the initial thickness.

As previously mentioned, four specimens were corroded and not tension loaded, so they remained intact. The noncorroded and corroded thicknesses could be measured both at the surface and in the notch. This demonstrated the different corrosion rates of the two areas.

CHAPTER IV

Results

4.1 Measured Fatigue Lives

The resulting fatigue lives of the specimens are listed below in Tables 4 and 5 and graphically represented in Figures 9 and 10. Table 6 compares the mean fatigue lives of each set of specimens to the baseline averages. These results identify an increase in the fatigue life of the specimens compared to either of the two baseline mean fatigue life values, 41,000 and 47,150 cycles.

Load	Specimen number			Average
index	1	2	3	life
1	48,437	69,926	69,971	62,778
2	39,346	45,178	53,189	45,904
3	42,283	56,033	56,193	51,503
4	41,039	52,403	60,557	51,333

Table 4. Fatigue lives of tested specimens, Exposure Index 1

Load	Specimen number			Average
index	1	2	3	life
1	40,788	40,708	44,358	41,951
2	54,419	55,890	59,814	56,708
3	39,015	57,797	59,134	51,982
4	41,856	47,607	53,410	47,624

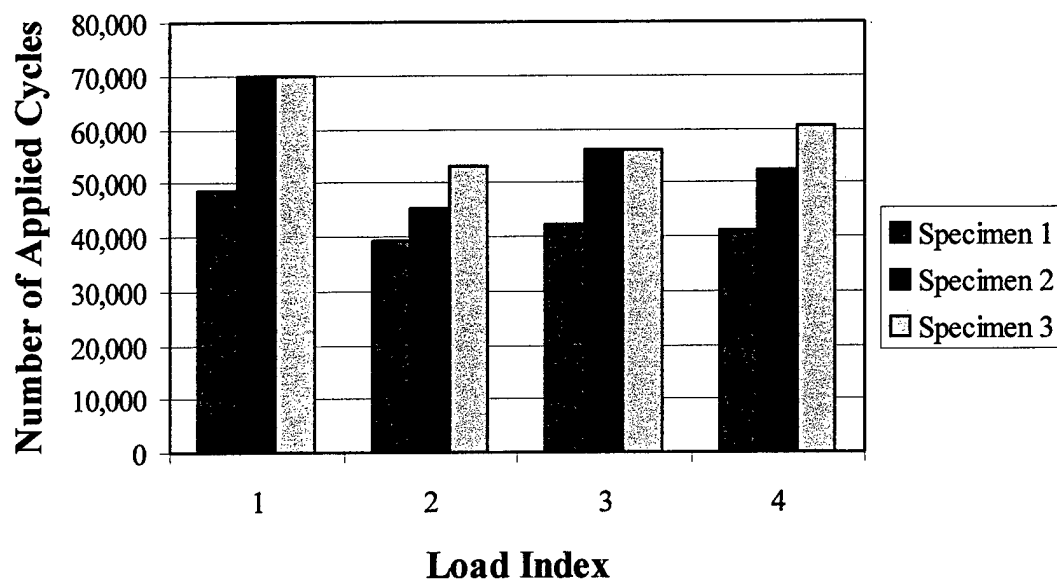**Table 5. Fatigue lives of tested specimens, Exposure Index 2**

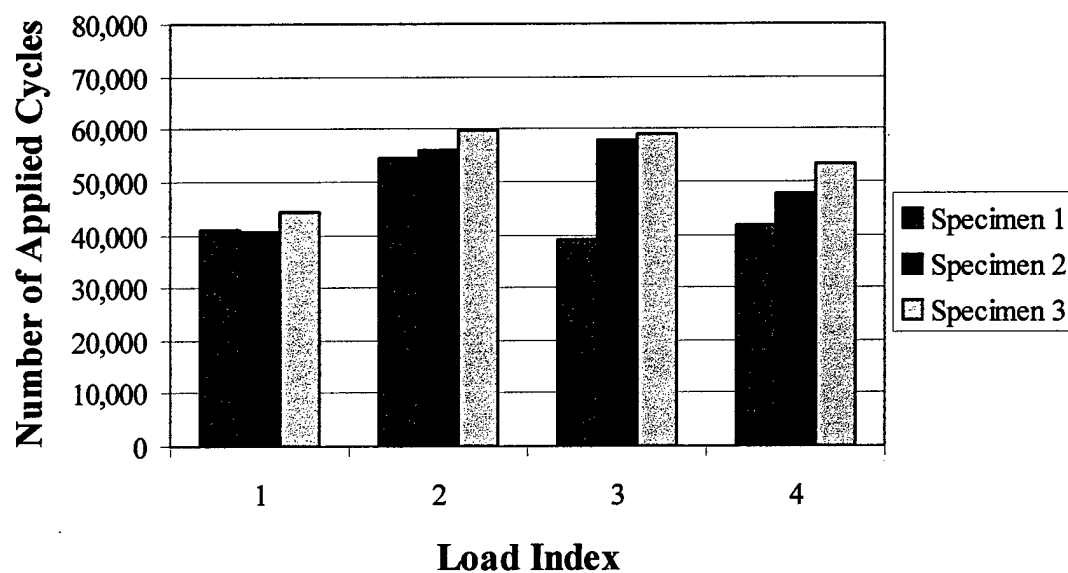**Figure 9. Fatigue life results for Exposure Index 1**

Figure 10. Fatigue life results for Exposure Index 2

Specimen Identification	Mean life (cycles)	% of 41,000 baseline mean	% of 47,150 Baseline mean
1-1-n	62,778	153%	133%
1-2-n	45,904	112%	97%
1-3-n	51,503	126%	109%
1-4-n	51,333	125%	109%
2-1-n	41,951	102%	89%
2-2-n	56,708	138%	120%
2-3-n	51,982	127%	110%
2-4-n	47,624	116%	101%

Table 6. Comparison of fatigue lives

4.2 Measured corrosion rates

In the areas of the notch and then fatigue cracks, the process of crevice corrosion occurred. Pitting, localized corrosion resulting in pits on the metal surface, could be observed in several areas including the notch. Uniform surface corrosion occurred on the exposed sections of the specimen, as is typical in corrosion cells without clearly defined anode and cathode surfaces (Mattsson 1989). The average depths of these corrosions represent the extent of the damage.

Corrosion rate can be determined by comparing corroded cross sections of members to their noncorroded cross sections. These measurements were taken at flat surface areas as well as within the notch. Due to the nature of failure, however, corrosion rates at the notch for failed members are not available. The section losses and corresponding cumulative corrosion times are presented below in Table 7 and Figure 11.

Specimen Identification	Total Hours	Thickness Loss (in.)	Corrosion Rate (in./hr.)	Corrosion Rate (mils/year)
Exposure Index 1				
1-1-1	482.5	0.0049	1.02E-05	88.96
1-1-2	642.5	0.0051	7.94E-06	69.53
1-1-3	642.5	0.0052	8.09E-06	70.90
1-2-1	642.5	0.0045	7.00E-06	61.35
1-2-2	802.5	0.0052	6.48E-06	56.76
1-2-3	962.5	0.0061	6.34E-06	55.52
1-3-1	1442.5	0.0060	4.16E-06	36.44
1-3-2	1762.5	0.0075	4.26E-06	37.28
1-3-3	1762.5	0.0086	4.88E-06	42.74
1-4-1	2562.5	0.0142	5.54E-06	48.54
1-4-2	3362.5	0.0129	3.84E-06	33.61
1-4-3	3842.5	0.0137	3.57E-06	31.23
Exposure Index 2				
2-1-1	234.5	0.0029	1.24E-05	108.33
2-1-2	234.5	0.0037	1.58E-05	138.22
2-1-3	306.5	0.0039	1.27E-05	111.46
2-2-1	522.5	0.0039	7.46E-06	65.39
2-2-2	522.5	0.0037	7.08E-06	62.03
2-2-3	522.5	0.0043	8.23E-06	72.09
2-3-1	666.5	0.0046	6.90E-06	60.46
2-3-2	954.5	0.0050	5.24E-06	45.89
2-3-3	954.5	0.0049	5.13E-06	44.97
2-4-1	1314.5	0.0067	5.10E-06	44.65
2-4-2	1458.5	0.0076	5.21E-06	45.65
2-4-3	1602.5	0.0099	6.18E-06	54.12
Control Specimens (surface)				
1	162.5	0.0024	1.48E-05	129.38
2	322.5	0.0038	1.18E-05	103.22
3	642.5	0.0061	9.49E-06	83.17
4	1282.5	0.0087	6.78E-06	59.42
Control Specimens (notch)				
1	162.5	0.0032	1.97E-05	172.50
2	322.5	0.0051	1.58E-05	138.53
3	642.5	0.0076	1.18E-05	103.62
4	1282.5	0.0102	7.95E-06	69.67

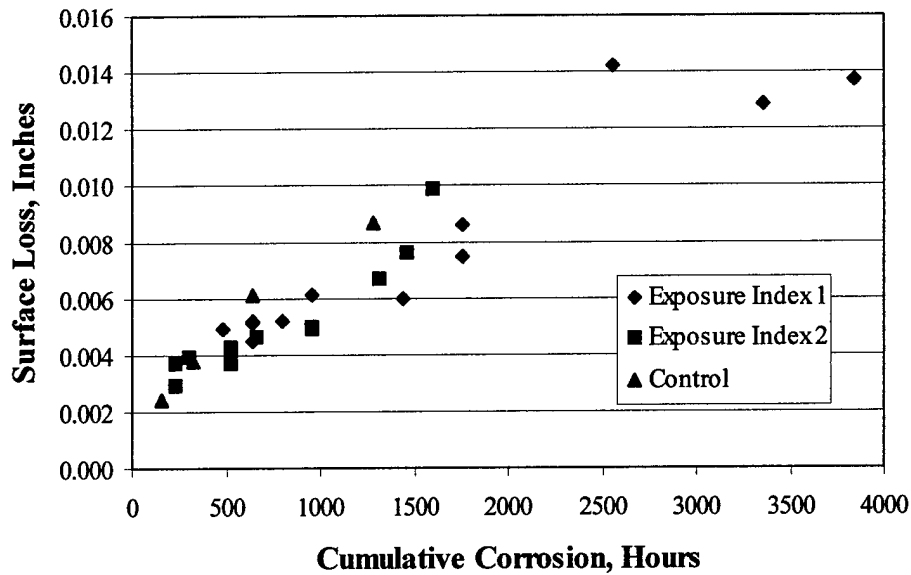**Table 7. Specimen section losses and corrosion rates**

Figure 11. Corrosion rates

Figure 11 graphically presents the corrosion rates of the different exposure

indices. As total corrosion exposure increases, there appears to be a decrease in the

corrosion rates.

4.3 Discussion of Results

4.3.1 Fatigue lives

The specimen in *exposure index 1, load index 1* experienced the largest increase

in mean fatigue life, a positive 53% increase. This large increase in fatigue life may be

attributed to the fact that in this short exposure time, the lack of corrosion of the cross-

section prevented any significant increase in the stress raiser created by the machined

notch and reduced cross-sectional area. The exposure time was enough, however, given the corrosion rate, to erode away any fatigue crack that initiated.

The specimens of *exposure index 2, load index 1* did not experience this same phenomenon as those of *1-1-n* (+2%). Such results can probably be attributed to their short corrosion exposure following the first load cycle. Either the fatigue crack initiated and propagated to critical depth during the second load cycle, or the crack initiated in the first load cycle and the 72 hour second period of corrosion did not counter fatigue crack initiation. They were apparently loaded such that the crack grew at a rate faster than the corrosion rate, so the fatigue crack was not deterred by corrosion. Once a crack has initiated and had time for any significant propagation, it is unlikely that anything short of severe corrosion will be able to keep up.

The average fatigue life of the *exposure index 1, load index 2* specimens was not as significant of an increase as those of *1-1-n* (only +12%). However, the specimens of *exposure index 2, load index 2* displayed a significant increase in fatigue life (+38%). It should be noted that the specimens of *2-2-n* were corroded for similar periods of time as those of *1-1-n*. This may indicate that between these two load-corrosion rates lies the most advantageous ratio to show an increase in fatigue life by corrosive consumption of the crack initiation. This does not mean, however, that such manipulation provides the most realistic model. Such information would confirm the hypothesis of corrosion "eating away" initiating fatigue cracks but would not provide realistic insight into the long-term, concurrent corrosion-fatigue relationship.

The specimens of *1-3-n* and *1-4-n* experienced a greater increase of fatigue life than those of *1-2-n* (+26% and +25%, respectively).

The mean fatigue lives of the remaining specimens in *exposure index 2* decreased from that of *2-2-n* but still out performed the control value. Those of *2-3-n* experienced an mean fatigue life 27% higher than the control, while those of *2-4-n* only realized and increase of 16%.

The variability of the results does not lend itself to accurate trend identification, but one trend appears clear: the mean fatigue life of the corroded specimens was greater than the mean fatigue life of the noncorroded specimens. Such results may dispel concerns that corrosion necessarily accelerates fatigue crack initiation in steel. In all fairness, though, such observation is based upon the mean control life of 41,000 cycles. This average did not incorporate the seemingly errant 66,427 cycle-life of one member. If this value were included in the calculation for mean control fatigue life, the value would be just over 47,150 cycles. Using this value, only 15 of the 24 specimens would have remained beyond 100% of the mean control fatigue life. However, the mean fatigue lives of all of the groups except *1-2-n* and *2-1-n* would still have been greater. Though not quite as convincing, the trend is still apparent.

In the field, the fatigue loading and corrosion would be simultaneous events. In this laboratory test, the two processes are not concurrent. For this reason, it is difficult to completely validate the comparison of corrosion rates versus crack initiation rates. Results of this test demonstrate the variability due this non-concurrence. Specimens *1-1-2* and *1-1-3* were corroded for 642.5 hours and experienced thickness losses of 0.0051and 0.0052 inch before failing at over 69,900 cycles. However, specimens *1-2-1* and *2-3-1*, with 642.5 and 666.5 hours corrosion exposure and 0.0045 and 0.0046 inch thickness losses respectively, both failed at just over 39,000 cycles. All of these specimens had

very similar times of exposure and thickness losses, but two experienced the greatest

fatigue life while two experienced the shorted fatigue life. Photographs of the failed

cross sections show the varying advance of corrosion over the total life of these
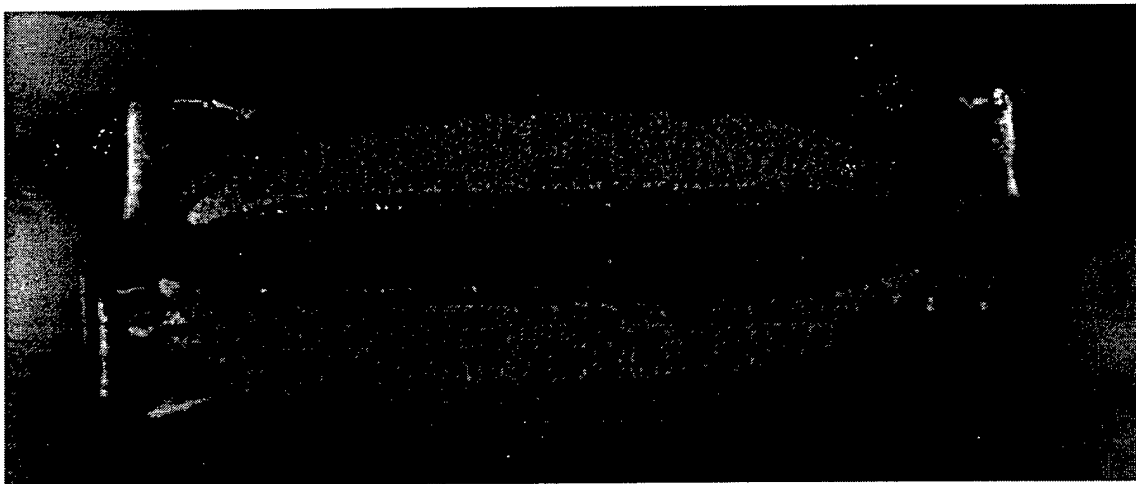
specimens (Figures 12 - 15).

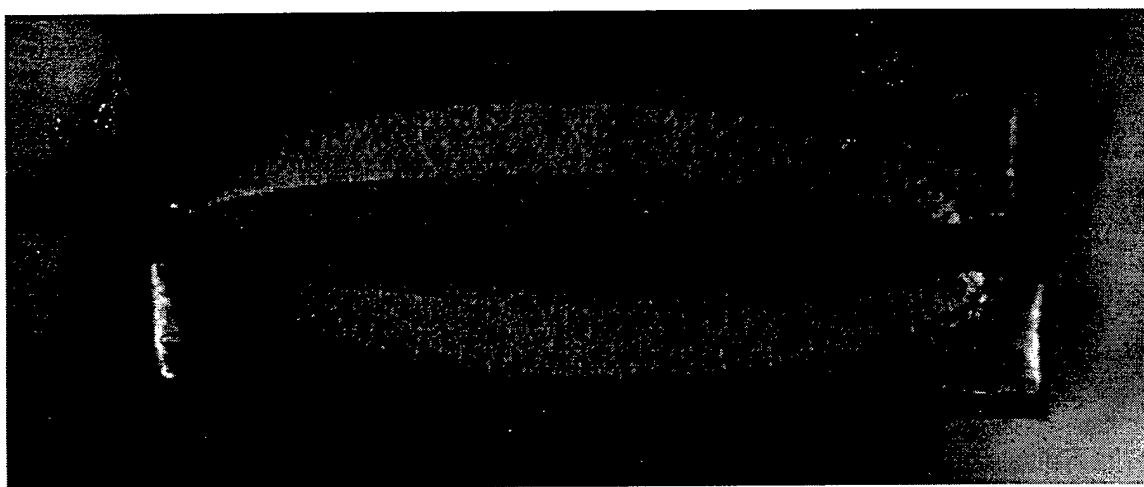**Figure 12. Failed cross section of specimen 1-1-2**

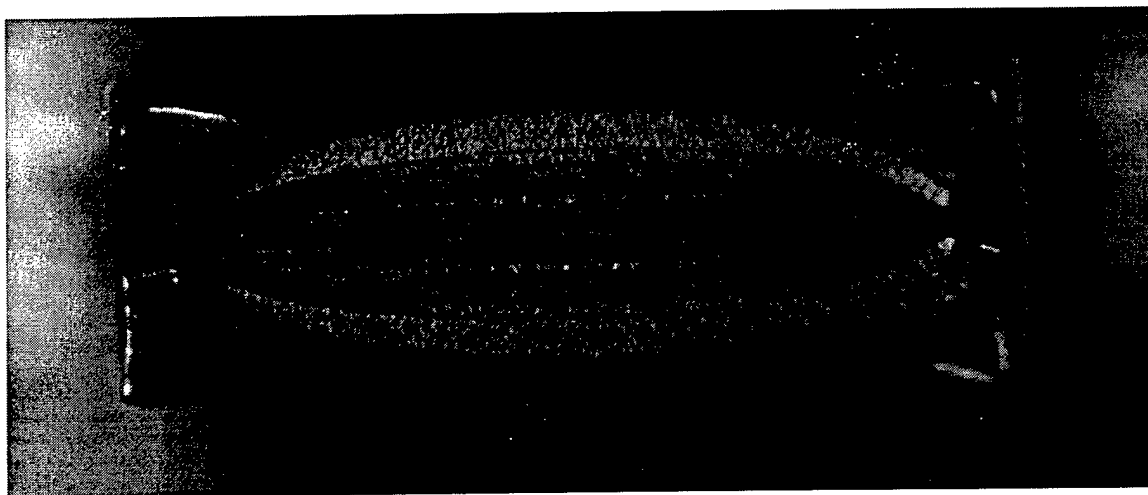**Figure 13. Failed cross section of specimen 1-2-1**

Figure 14. Failed cross section of specimen 2-3-1

4.3.2 Corrosion rates

Several aspects of the set-up of this test environment help to provide a "neutral" setting. Extreme pH levels can affect the corrosion rates of steel in a saline solution. However, for near-neutral conditions ($5<pH<9$), pH no longer plays a direct role in corrosion rates. Additionally, in neutral pH ranges, the presence of oxygen inhibits direct correlation of iron corrosion with chloride ion concentration. The circulating air pump assists in the maintenance of oxygen levels. This is particularly important due to the decreased solubility of oxygen in salt water.

The corrosion rates measured at the notch were greater than those measured at the surface. This phenomenon is due to crevice corrosion as described in Chapter 2.

As cracks initiated in the notches of the specimens, corrosion was allowed to penetrate into the specimen. With every growth in crack depth, corrosion penetrated

further. Photographs of the failed cross sections in Figures 12-14 document the result of this process showing the stratification of levels of corrosion.

The four control specimens corroded without load demonstrate the effects of corrosion on the surface (Figures 15-18) and provided information to compare corrosion rates in the notches and on the surfaces. Progression from one week to eight weeks produces an obvious increase in uniform corrosion as well as pitting.
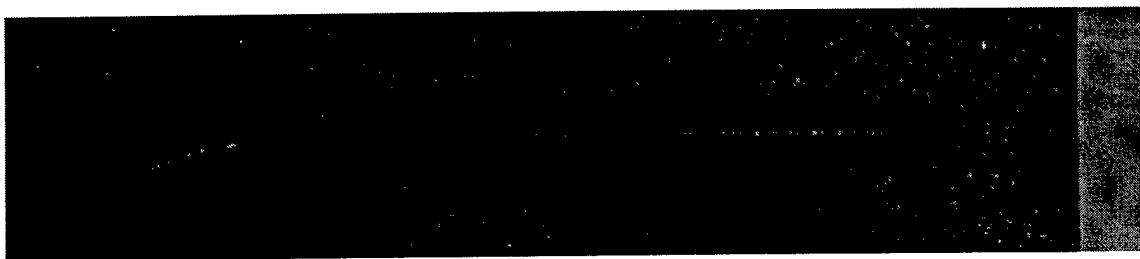

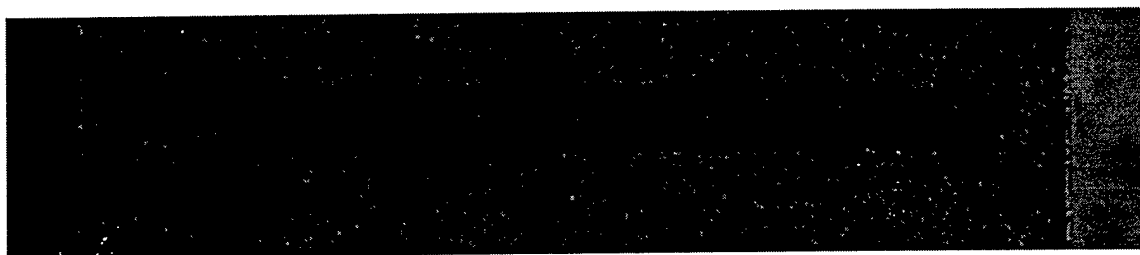**Figure 15. Corrosion control specimen 1 (1 week)**

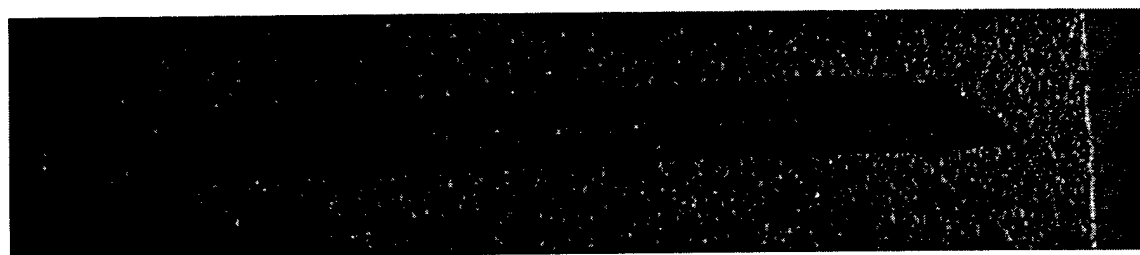**Figure 16. Corrosion control specimen 1 (2 weeks)**

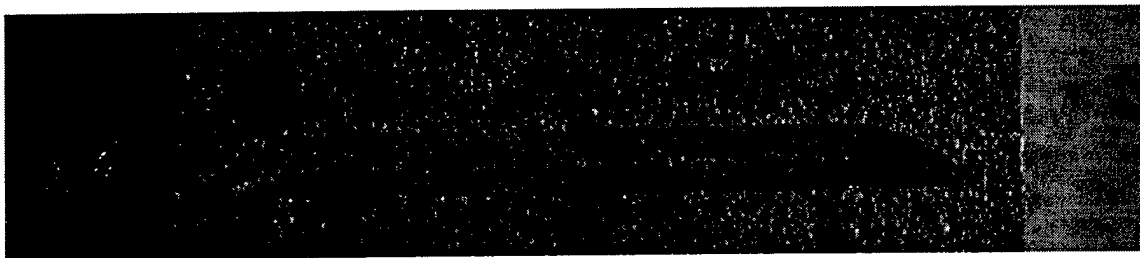**Figure 17. Corrosion control specimen 3 (4 weeks)**

Figure 18. Corrosion control specimen 4 (8 weeks)

If one specimen was continuously exposed to a saline solution environment for a long period of time and periodic loss measurements taken, it is likely that the corrosion rate curve would be a function of the square root of time. The rate of corrosion is not linear as it decreases with the development of a protective film produced from the corrosion process. If this protective film were continually removed, the corrosion rate would be allowed to more closely represent a linear function with respect to time. As such, it should be expected that all of the specimens of an exposure index should have similar linear rates of corrosion. In this study, however, there appears to be a general trend of decreasing corrosion rates with increasing cumulative corrosion hours. The relationship is close to being a function of the square root of time: $0.0002t^{0.53}$ as determined by a regression analysis of the data in Figure 11 (with an R-value of 0.8913). Much of the protective layer was continually brushed off throughout the corrosion cycles, however the oxidized layer is not so easily removed and enough of the protective layer remained intact to maintain a relationship with the square root of time.

The downward trend observed in corrosion rates also appears to compliment a decreasing trend in specimen fatigue lives. It is possible that the decrease in corrosion rates allowed the crack initiation rate to prevail in this microscopic race.

4.3.3 Load eccentricity

Another factor that could affect the fatigue life was the eccentricity of the applied load due to the geometry of the specimens. The calipers applying the tension load gripped the specimen at a full cross section. However, the fact that the specimen was notched on only one side created an eccentricity of the load. With every corrosive interval, the depth of the notch grew, increasing this eccentricity. Compounded with the propagating notch, the surface on the side of the notch had been sand blasted which allowed for surface corrosion. The surface on the side of the notch corroded with every interval and also increased the eccentricity of the load. As the test progressed the increasing eccentricity of the tension loads progressed to a point where the test equipment shuddered during the application of cyclic loads.

4.3.4 Notch Pitting

The pitting action in the notch is apparent from the discontinuities of the rust advance lines at the notch in the failed cross section below (Figure 19). As pitting corrodes away the specimen, most critically at the notch tip, the stress concentration is increased due to the geometric irregularity. The net effect is an increase of stress across the thinnest portion of the specimen, which facilitates fewer load cycles to failure.
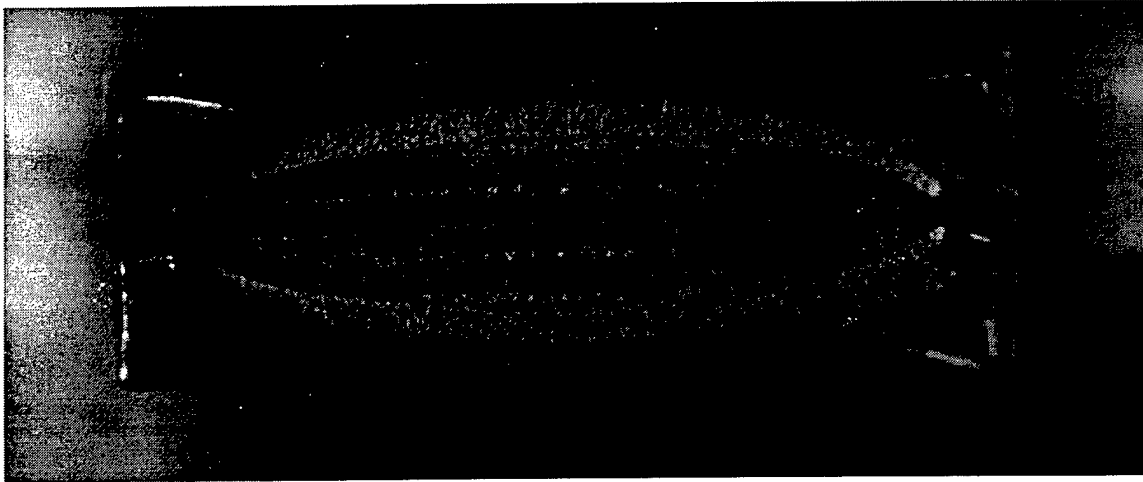
Figure 19. Notch pitting

4.3.5 Section Loss on Surface

As the surface corrodes, the cross sectional area decreases. The stress range in a specimen equals the change in force divided by the area. With any decrease in cross sectional area, there is an increase in the stress range. In fact, an increase in the stress range typically decreases the fatigue life as demonstrated in the following equation:

$$N_f = \frac{A}{\Delta\sigma^{3.0}}$$

where N_f is the number of cycles at fatigue life failure, A is area, and $\Delta\sigma$ is the stress range. For example, a thickness loss of 0.0109 inches provides a 7% loss of the cross sectional area of the specimen. This 7% loss will directly affect N_f, decreasing it by 7%. The 7% decrease in area will also increase the stress range by 7.5%. When this value is cubed in the denominator, it decreases Nf by 20%. The combination of these two effects is a net decrease in fatigue life of 25%.

CHAPTER V

Finite Element Analysis of Stress-raiser

5. 1 Finite Element Model (FEM)

The determination of stresses at the notch of this steel specimen can be accomplished using a finite element model and computer processing using ABAQUS and PATRAN. In order to do this, some simplifications and some approximations must be made to model the system. The geometry of the specimen as entered into ABAQUS and PATRAN is presented below as Figures 20 and 21. Using symmetry, only one half of the specimen must be analyzed from the centerline of the notch. The modeled specimen measured only 0.0720" from the centerline of the notch. At this point, it is safe to assume that the stress distribution returned to nearly uniform and is of not consequence when focusing on the notch. The modeled specimen height (0.1844") corresponds to the uncorroded thickness of Control Specimen 4 and is more accurate than the nominal 3/8" thickness. The thickness of the member into the page was taken as a "unit" thickness of 0.01" to represent any point of the specimen along the notch. Two geometries, each with 3150 elements, were considered representing the specimen before exposure to the corrosive environment and after 8 weeks of exposure. These elements were eight-noded quadratic elements. Only the corrosion at the notch was accounted for in the FEM computer model. The difference in surface thickness can be readily computed by hand and applied to the results.
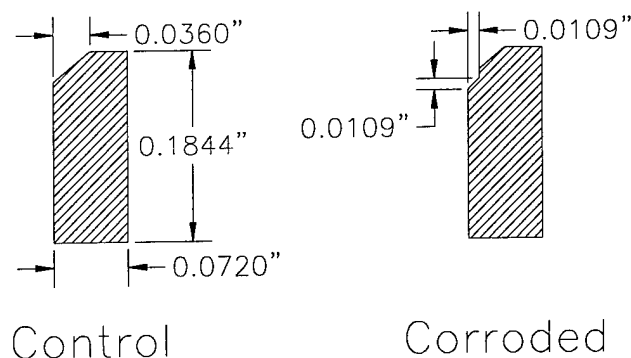
Figure 20. FEM geometries

The member is modeled as having roller boundary restraints at the left edge—the interface of specimen symmetry. It is not allowed to deflect horizontally, but it is allowed to deflect vertically. This provides the specimen with the capability of necking due to the axial load. A pinned connection at the lower left corner maintains static equilibrium. Since the vertical "centroids" of the applied force and resistance are not equal, a moment is created. Unrestrained, the right end of the specimen model will deflect vertically from this resultant moment. If the entire specimen had been represented, equilibrium would have balanced these non-concentric forces. Since only one side is modeled, it is necessary to impose boundary conditions to simulate total equilibrium. This is accomplished by providing rollers to the bottom of the specimen to keep it from deflecting vertically (Figure 21). A 1000 pound/in distributed load was applied to the right side. This also provides for easy manipulation of the results.
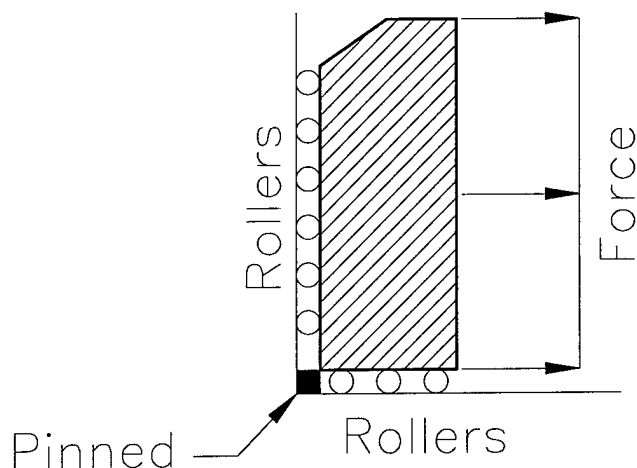
Figure 21. FEM boundary conditions

For this study, the two models were created using PATRAN and ABAQUS computer programs. As a general rule, PATRAN was used to set up the complex meshes and develop initial input files. Once input files were generated, ABAQUS was used to complete the finite element computations.

5.2 FEM Results

Predictably, the stress concentration at the face of the corroded notch is higher than the stress at the interior notch face before corrosion. This effect is highly localized in nature. The stress gradient plots of the notch area in Appendix B illustrate the difference visually. Compensating for a surface loss of 0.0087 inches, the difference in maximum stress at the edge is a factor of 1.3. If it is assumed that the entire cross section of the specimen is the same geometry, then the units of this model are irrelevant and only the ratios and factors are of significance as they can be applied to any load within an elastic range.

Since the edges of the notch are not the same as the center length of the notch, the assumption of plane strain is not totally accurate. However, the scale of error is small enough to overlook in this circumstance.

CHAPTER VI

Conclusions

6.1 Test Procedure

The results of testing demonstrate mean corroded fatigue lives greater than that uncorroded. Due to the difficulty in determining the actual crack initiation, it is assumed that retardation in fatigue failure is primarily a result of a delay of the onset of crack initiation. This is an appropriate and reasonable assumption as none of the corrosion characteristics should significantly deter crack propagation associated with tension perpendicular to the propagating crack. The results of testing certainly support the possibility that corrosion consumes initiating cracks as demonstrated by the increased fatigue lives. However, the testing process needs to be refined in order for more conclusive evidence to be realized.

6.2 Implications

The results of this investigation combined with the presented mathematical investigation demonstrate that corrosion can actually deter the initiation of fatigue cracks, thereby increasing the mean fatigue life of these specimens. These results identify that a reduction in AASHTO fatigue design limits may be premature. As such, unnecessary reduction in fatigue lives would require increased funding to repair structures that may not require such actions.

6.3 Need for Further Investigation

Despite the straightforward mathematical presentation, and the given fatigue resistance of serviceable structures, more information is still necessary. "Sufficient data are available to show the existence of a fatigue-crack-propagation threshold, ΔK_{th}, below which existing fatigue cracks do not propagate under cyclic loading. However, more work is needed to understand better the effects of various factors on the magnitude and the existence of ΔK_{th} and to use it properly in design" (Barsom 1987).

As a result of this study, some specific recommendations may aid in future endeavors:

1. Provide simultaneous corrosion and loading process, or at least closer to this ideal situation by decreasing the percent loading between corrosive periods

2. Attempt to match predicted corrosion rates with crack initiation rates

3. Utilize a larger number of test specimens with less conditions to better identify trends.

6.4 Summary

Evidence suggests that in low stress cyclic loading the onset of fatigue crack initiation may be delayed due to corrosion. This delay in crack initiation precedes design life of the structure beyond that predicted by AASHTO codes. While more tests need to be accomplished to determine the exact effect of corrosion of fatiguing steel, reduction factors to AASHTO code recommended appear premature, and possibly even unnecessary.

REFERENCES

Albrecht, Pedro, "Fatigue Design Stresses for Weathering Steel Structures," *Corrosion Fatigue: Mechanics, Metallurgy, Electrochemistry, and Engineering, ASTM STP 801*, pp. 445-471, 1983.

Barsom, John M. & Stanley T. Rolfe, <u>Fracture and Fatigue Control in Structures</u>, 2nd ed., 1987.

Boresi, Arthur P., Richard J. Schmidt & Omar M. Sidebottom, <u>Advanced Mechanics of Materials</u>, 5th ed., 1993.

Fisher, J., "Fatigue Resistance of Weathering Steel Components", Forum on Weathering Steel for Highway Structures: Summary Report, June 1989.

Harrison, J.D, "An analysis of data on non-propagating fatigue cracks on a fracture mechanics basis," *Metal Construction and British Welding Journal*, March, 1970.

Mattsson, Einar, <u>Basic Corrosion Technology for Scientists and Engineers</u>, 1989.

Ohta, Akihiko, Takeshi Kono, & Satoshi Nishijima, "Near-threshold Fatigue Crack Propagation of Welded Joint Under Varying Loading," *Engineering Fracture Mechanics* Vol. 21, No3, pp. 521-528, 1985.

Wright, William J., & Pedro Albrecht, "Fatigue Crack Growth Rates in Bridge Steels," *Transportation Research Record 1290.*

APPENDIX A

Nomenclature

The following symbols are used in this paper:

a = crack depth

da/dN = rate of crack growth , inches per load cycles

K = stress intensity factor

K_{Ic} = critical stress-intensity factor

K_{max} = maximum stress-intensity factor

ΔK = stress-intensity fluctuation

ΔK_{th} = threshold stress-intensity fluctuation

N = number of load cycles

$(N_f)_{mean}$ = mean number of load cycle to failure

$N_{interval}$ = interval number of cycles
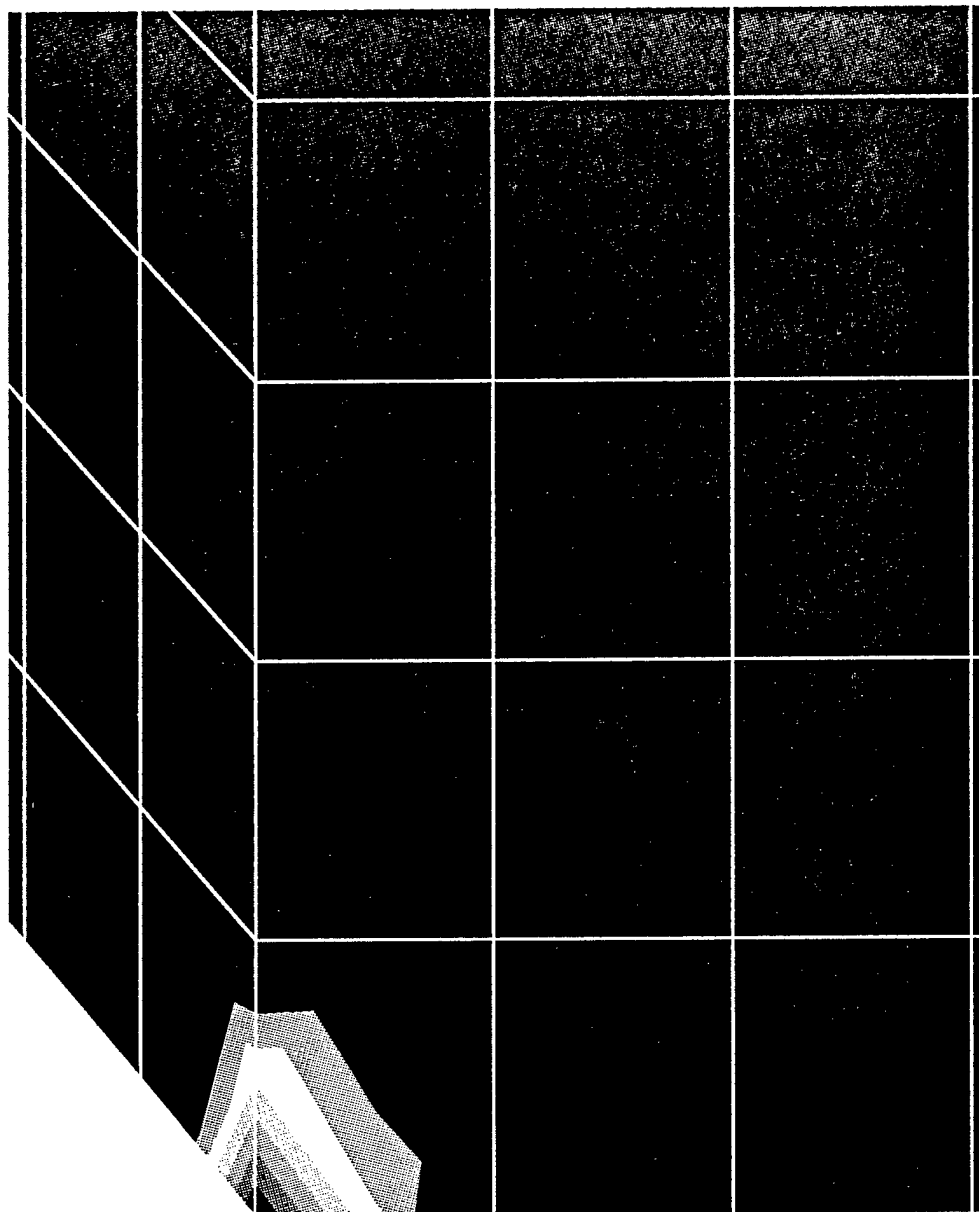
$\Delta \sigma$ = range of normal stress

APPENDIX B

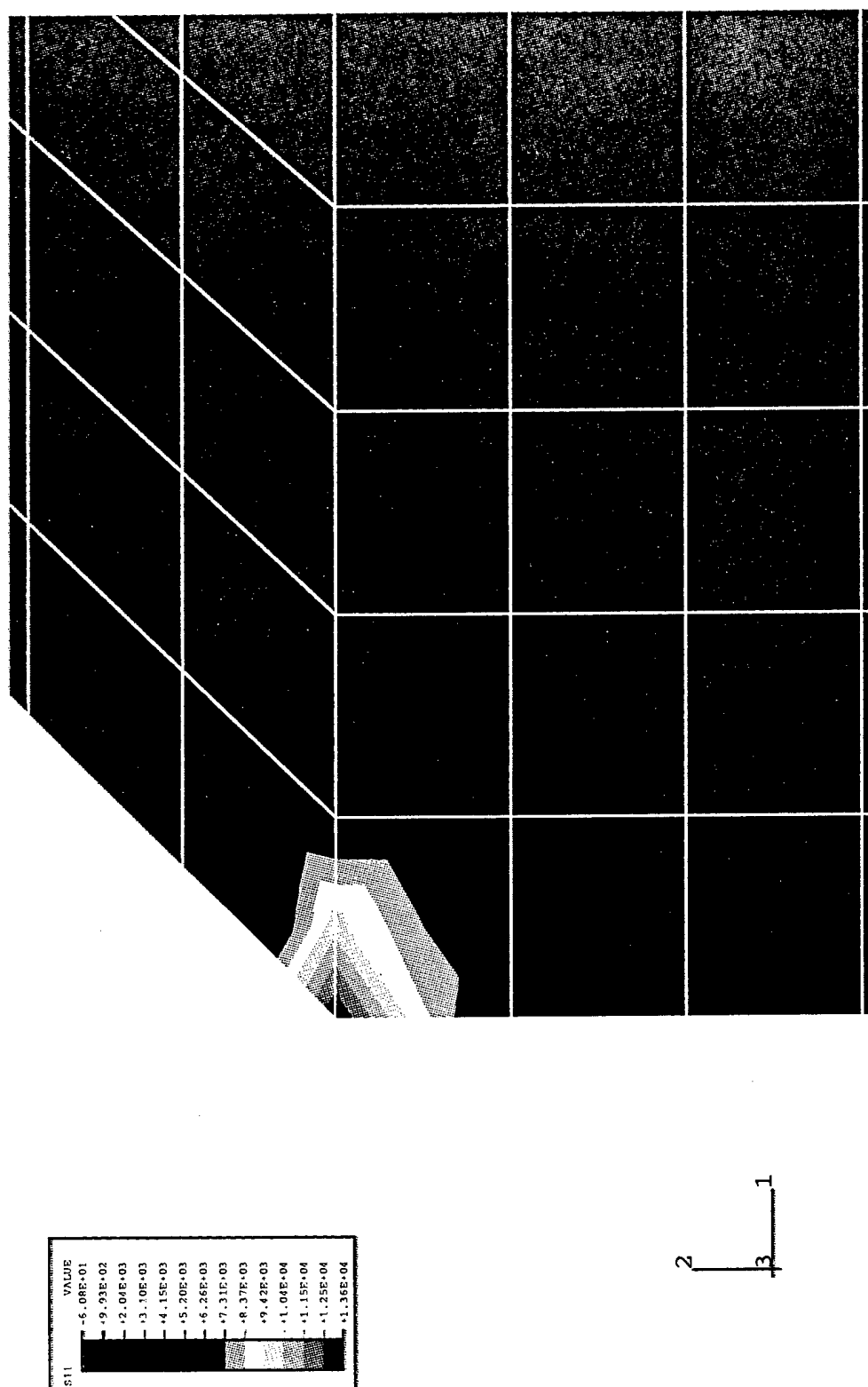
Figure B1. Stress gradient, uncorroded geometry

Figure B2. Stress gradient, corroded geometry

VITA

Todd S. Waldvogel
32 Gannet Hollow Place
The Woodlands, Texas 77381

EDUCATION   **Texas A&M University**, College Station, Texas
Master of Engineering in Civil Engineering, August 1997

United States Air Force Academy, Colorado Springs, Colorado
Bachelor of Science in Civil Engineering, May 1992